AE-179
UDC 539.144.6

AE-179

Hindered E1 Transitions in Eu^{155} and Tb^{161}

S. G. Malmskog

AKTIEBOLAGET ATOMENERGI
STOCKHOLM, SWEDEN 1965

HINDERED E1 TRANSITIONS IN Eu^{155} AND Tb^{161}

Sven G. Malmskog

Abstract

The absolute E1 transition probabilities from the $\frac{3}{2}+(411)$, $\frac{5}{2}-(532)$ and $\frac{7}{2}-(523)$ single particle levels in Eu^{155} and Tb^{161} have been measured by the method of delayed coincidences. This gave half lives of $T_{1/2} < 0.2$ ns and $T_{1/2} = (1.38 \pm 0.06)$ ns for the 104.4 and 246 keV levels in Eu^{155}, $T_{1/2} = (0.84 \pm 0.04)$ ns and $T_{1/2} < 0.2$ ns for the 417.6 and 480.6 keV levels in Tb^{161}. The result has been compared with the calculations of a single particle in a deformed potential made by Nilsson.

Printed and distributed in February 1965.

LIST OF CONTENTS

1.0 Introduction

It has been well demonstrated that E1 transition rates in the region of deformed nuclei are strongly hindered as compared with the single proton estimate by Weisskopf [1]. To some extent these facts are understood in the light of the calculations made by Nilsson [2], who considered the individual particle motion in a deformed potential. Recently it has been pointed out [3] that both the pairing correlation and the giant dipole resonance can strongly influence the E1 transition probabilities. It is therefore of importance to compare experimental E1 transition probabilities with theoretical calculations to try to understand the influence from the different co-operating factors. The measurements of absolute E1 transition probabilities between identical single particle levels in adjacent odd-mass nuclei is also a sensitive test of the influence exerted on the particle motion when an even number of protons or neutrons are added to the nucleus.

In this paper an experimental study of some absolute E1 transition probabilities in Eu^{155} and Tb^{161} is performed. The result is compared with the predictions from the Nilsson model.

2.0 Experimental procedure

2.1 Apparatus

A fast-slow coincidence apparatus supplied with NE-102 plastic scintillators optically coupled to 56 AVP photomultipliers was employed. Throughout these experiments the γ- rays were detected by a $1.5'' \times 1''$ scintillator while for β registration a $1.5'' \times 1$ mm scintillator was used. The total system had a time resolution with a width at half maximum of 0.6 ns using a Co^{60} source. Calibration of the time-to-pulse-height converter was performed against the velocity of light in air to within 0.5 per cent using a fast light-pulse generator. All details of the experimental set-up and the time calibration have been given elsewhere [4].

2.2 Sources

All the activations have been made at a neutron flux of 10^{12} n/cm^2 · sec in the Research Swimming-Pool Reactor R2-0 at Studsvik.

Samples of highly enriched Sm^{154} (99.2 per cent) were used. From a mass analysis small amounts of Sm^{152} (0.4 per cent) and Sm^{149} (0.2 per cent) were found. No other impurities with more than 0.05 per cent were detected. A scintillation spectrum showed no other activity than the one belonging to the Sm^{155} decay.

The gadolinium sources were made from spectroscopically pure Gd_2O_3. The only short-lived activity observed was Gd^{161} (3.7 min). After several activations a background of Gd^{159} and Tb^{161} was observed. To diminish this background each Gd source was exchanged after 10 reactivations.

2.3 Treatment of experimental data

If the lifetime of an energy level is of the order of the width at half-maximum of the corresponding prompt resolution curve or longer, a convenient way to obtain $T_{1/2}$ is through a least squares fit. The number of measured delayed coincidences from a single decay "y" as a function of the channel number "x" is given by [4].

$$y = \int_k^\infty A\lambda e^{-\lambda(u-k)} \cdot \frac{1}{\sigma\sqrt{2\pi}} \exp\left[-\frac{1}{2}\left(\frac{x-u}{\sigma}\right)^2\right] du + B \quad (1)$$

where A is the area of the delayed curve, λ the decay constant, σ the standard deviation and B the background. From a least squares fit between eq. (1) and the experimental time coincidence distribution, λ and thus $T_{1/2}$ is determined together with its standard deviation.

When the lifetime is much shorter than the prompt time resolution the method of momentum analysis can be used. It has been shown [5] that the mean life of the delayed transition can be obtained from the difference between the momentum of the delayed and a prompt distribution both taken under the same experimental conditions. Information on the mean life can also be obtained from higher momenta but with less statistical accuracy [5]. A program has been constructed which calculates the first three momenta of the delayed and prompt distributions and, from them the mean life of the delayed level for each momentum together with its standard error.

3.0 Experimental data

3.1 104 keV level in Eu^{155}

After Pool and Quill [6] in 1938 had observed a twenty-one minute activity in samarium, several complementary investigations have been made [7 - 11]. Recently Kracik et al. [12] have reinvestigated the decay of Sm^{155} using an intermediate image magnetic lens and a NaI(Tl) spectrometer. Besides the three well-known gamma rays they found eleven new weak lines extending from 450 keV to 1440 keV. A simplified decay scheme is shown in fig. 1.

According to the Nilsson diagram the ground state assignment for a nucleus with 63 protons is $\frac{5}{2}+(413)$ assuming a deformation of $\delta \approx 0.3$. This is in agreement with the measured spin and parity $\frac{5}{2}+$ for the ground state in Eu^{153}. From the conversion coefficients $\alpha_K \approx 0.27 \pm 0.06$ from Schmid and Burson [9] and $\alpha_K \approx 0.37 \pm 0.09$ and $\alpha_L \approx 0.057$ from Kracik et al. [12], it is concluded that the 104 keV line is predominately E1 with a M2 mixture of less than two per cent. This information together with the selection rules imposed by the β^- decay from Sm^{155} gives a spin and parity of $\frac{3}{2}-$ or $\frac{5}{2}-$ for the first excited state. The closest Nilsson level with negative parity and suitable spin is the $\frac{5}{2}-(532)$ orbit which is identified with the 104 keV level. This orbit is known to be the ground state of Eu^{151} and the first intrinsic level in Eu^{153}. For large deformations ($\delta \sim 0.3$) the $\frac{5}{2}-(532)$ orbit is well below the $\frac{5}{2}+(413)$ ground state orbit but approaches this for smaller deformations ($\delta \sim 0.2$). This fact, together with the observed weak feeding by the allowed but hindered β^--transition to the 98 keV $\frac{5}{2}-(532)$ level in Eu^{153} (log ft $\approx$ 8.6), is taken as evidence of a small eccentricity of the 98 keV level. The E1 transition to the ground state is then expected to be slowed down as a consequence of the asymptotic selection rules and the change of nuclear equilibrium [13]. A recent measurement [16] gives a half-life of $(1.58 \pm 0.21) \times 10^{-10}$ sec for the 98 keV level in Eu^{153}. In Eu^{155} the allowed but hindered β^--transition to the 104 keV $\frac{5}{2}-(532)$ level has an unusually low value of log ft $\approx$ 5.7. This indicates that the change in the nuclear equilibrium is not so large for this transition as for the similar one in Eu^{153} and that the subsequent E1 transition is less retarded.

We have measured the lifetime of the 104 keV level in Eu^{155} by recording the delayed coincidences between the feeding beta and the 104 keV gamma transition. The result was obtained by the method of momentum analysis [5]. To determine the prompt resolution curve, we used the prompt levels in Fe^{56} (845 keV, 7 ps), Se^{76} (559 keV, 12 ps) and Te^{122} (564 keV, 8 ps) without changing the energy windows. For each isotope five different distributions were measured. From the determination of the position of the centroid of each distribution from the first momentum (against an arbitrary zero), average values for each isotope were obtained as Eu^{155} (2.82 ± 0.03 nsec), Fe^{56} (2.92 ± 0.03 nsec), Se^{76} (2.95 ± 0.03 nsec) and Te^{122} (2.85 ± 0.04 nsec). The last three isotopes are all known to be prompt, but still there is disagreement with the result for the first momentum of the prompt curve. This may be due to electronic instability, variations in source strength and position, different energy distributions in the rather large, fixed energy-selective windows used, and so on. There are many reasons for getting a small time shift of the order of 0.1 nsec, and a careful technique has to be used to take care of them all.

The mean life of the 104 keV level can now be obtained from the difference between the first momenta of the delayed and the prompt curves. From the Eu^{155}, Fe^{56} and Se^{76} values a mean life of the order of 0.1 nsec is suggested, but Te^{122} indicates a smaller value. We have also calculated the second and third momenta for all time distributions. Although the statistical errors are higher for these momenta [5] they indicate a mean life between 0.1 - 0.2 nsec. From most of the data a half life about 0.1 nsec is indicated for the 104 keV level, but the absolute value is rather uncertain. It is possible, however, to definitely establish a half life less than 0.2 nsec for this level. Compared with the Weisskopf single proton estimate [1] this gives a retardation factor of $< 2 \cdot 10^3$.

3.2 246 keV level in Eu^{155}

The 246 keV level is known to decay by two gamma rays of 142 keV and 246 keV to the first excited and the ground state (fig. 1). There intensity ratio $\frac{I_{246}}{I_{142}}$ has been measured by Schmid and Burson [9] (≈ 5.2), Sund, Arns and Wiedenbeck [10] (≈ 2.5) and Kracik et al. [12] (≈ 2.2).

From a scintillation spectrum taken from a Sm^{155} source we estimated the $\frac{I_{246}}{I_{142}}$ gamma intensity ratio to be 2.4 ± 0.3. A K-conversion coefficient of $\alpha_K = 0.16 \pm 0.06$ has been measured for the 142 keV transition by Schmid and Burson. This shows that the 142 keV transition is predominantly E1 with a M2 content of less than two per cent.

The nature of the 246 keV transition is, however, not so certain. Rutledge et al. [8] gave as a rough estimate a value of $\frac{K}{L} \approx 8$. This indicates a M1 transition. The more recent conversion coefficient measurement by Kracik et al. [12], however, gives a value of $\frac{K}{L} = 5.3 \pm 2$, which gives M1 with E2 admixture. Owing to the reported large errors, no definite value for the E2 content in the 246 keV transition can be made. The conversion coefficients for the corresponding 103 keV transition in Eu^{153}, however, have been accurately measured by Suter et al. [14]. Using the $\frac{L_1 + L_2}{L_3}$ ratio they determined an E2 admixture of 1.1 per cent. From this analogy, the 246 keV transition in Eu^{155} is believed to be predominantly M1. The multipole assignments together with selection rules for the β^- decay of Sm^{155} give $\frac{3}{2}+$ $\frac{5}{2}+$ for the 246 keV level. As the $\frac{3}{2}+(411)$ orbit is expected to give a low lying state in Eu^{155}, the $\frac{3}{2}+$ assignment is favoured. This orbit is also known to be the second excited intrinsic state in Eu^{153}. With the $\frac{3}{2}+(411)$ assignment for the 246 keV level both the 142 keV E1 and 246 keV M1 transitions are forbidden by the selection rules for the asymptotic quantum numbers [13].

The delayed time coincidence spectrum between the β^- and the 246 keV γ-transition has been measured. The β^- window was set to accept the energy interval 800-1000 keV, while the γ window was adjusted to exclude the influence from the 104 keV transition. The result is shown in fig. 1. The prompt part of the time distribution orginates from β-γ coincidences from higher energy gamma transitions in Sm^{155}, first observed by Kracik et al. [12]. The influence of these higher gamma transitions can be reduced by increasing the lower β^- energy level, but that will be at the sacrifice of a lower coincidence rate. In analysing the result a fraction of an experimentally determined prompt coincidence curve was subtracted from the delayed curve until the best least squares fit with eq. (1) was obtained.

From such an analysis of six measured time distributions a half life of (1.38 ± 0.06)ns was obtained for the 246 keV level in Eu^{155}. Compared with the Weisskopf single particle estimate [1] this gives retardation factors of 7×10^4 and 10^3 for the 142 keV E1 and the 246 keV M1 transitions respectively.

3.3 418 keV level in Tb^{161}

Ninety per cent of the β^- decay from Gd^{161} is populating the 417.6 keV level (fig. 2). This level decays by three gamma rays with energies of 102.4 keV, 283.8 keV and 361.0 keV to the first excited intrinsic level (315.3 keV), the second and first rotational levels being built on the ground state. According to Schmid, Burson and Cork [15] all these three transitions have E1 multipolarity with small M2 admixture, as is indicated by their K-conversion coefficients of 0.22, 0.041 and 0.018 resp. The ground state of Tb^{161} with 65 protons is predicted by Nilsson [2] to be a $\frac{3}{2}+(411)$ configuration. This is in agreement with the measured spin $\frac{3}{2}$ for Tb^{159}. The E1 character of the 283.8 and 361.0 keV γ-rays above gives a spin of $\frac{5}{2}$ or $\frac{7}{2}$ with negative parity for the 417.6 keV level. From the allowed unhindered character ($\log ft \sim 5.0$) of the β^- transition from the $\frac{5}{2}-(523)$ ground state of Gd^{161} to the 417.6 keV level, this state is taken to be the $\frac{7}{2}-(523)$ intrinsic level which is expected at about this excitation energy. This implies that the 283.8 keV and 361.0 keV E1 transitions are once K-forbidden ($|K_i - K_f| = \lambda + 1$). The delayed time coincidence spectrum between the 1.60 MeV β-transition and the 361.0 keV γ-transition has been measured. After some reactivations of the source it was found that the background activity from Gd^{159} (18.0 h) and Tb^{161} (6.9 d) increased. To avoid the influence from these decays the β^- window was placed high enough not to admit the 0.59 MeV β^--transition from Gd^{159} and the γ-window was adjusted to get a negligble influence from the 315.3 keV transition in Tb^{161}. Furthermore each source was replaced after ten irradiations. A small coincidence rate from γ-rays in Tb^{161} with energies higher than 360 keV is, however, unavoidable. Its effect has been estimated and corrected for. The result is shown in fig. 2. The delayed curves have all been analysed by a least squares fit to eq. (1) and with the momentum method.

From the analysis with both methods on seven delay curves a mean value of 0.84 ± 0.04 ns was obtained for the half life of the 417.6 keV level in Tb^{161}.

Compared with the Weisskopf estimate [1] this gives retardation factors of 3×10^4, 9×10^5 and 2×10^5 for the 102.4 keV, 283.8 keV and 361.0 keV E1 transitions, respectively.

3.4 481 keV level in Tb^{161}

A weak β^--branch (7 per cent) is populating the 480.6 keV level which decays by two gamma rays of 165.3 keV and 481 keV to the first excited intrinsic level (315.3 keV) and the ground state. The K-conversion coefficient for the 165.3 keV transition ($\alpha_K \approx 0.097$) indicates a E1 multipolarity with small M2 mixing. The M1 character of the γ-transitions from the 315.3 keV level in Tb^{161} to the ground state rotational band [15] gives $\frac{3}{2}$ or $\frac{5}{2}$ spin and positive parity to this level and is identified with the $\frac{5}{2}+(413)$ configuration. The 165.3 keV E1 transition to this level gives $\frac{3}{2}$, $\frac{5}{2}$ and $\frac{7}{2}$ as possible spins for the 482 keV level together with negative parity. This level is taken as the $\frac{5}{2}-(532)$ configuration which is the only odd parity intrinsic state expected in this energy range. This configuration is also known to give lowlying excited states in Eu^{153}, Eu^{155}, Tb^{155}, Tb^{157} and Tb^{159}. It is also known that the ground state transition from the $\frac{5}{2}-(532)$ level in Tb^{155}, Tb^{157} and Tb^{159} is by far the strongest transition to the ground state rotational band. This agrees with the present assignment of the $\frac{5}{2}-(532)$ level in Tb^{161}, as the 481 keV ground state transition is the only one observed. The allowed hindered character of the β^--transition populating the 481 keV level given by the above assignments is in agreement with the observed log ft $\sim$ 6. From this decay scheme it now follows that the 481 keV transition is E1 with a low M2 mixing as obtained by comparison with the corresponding transition in other odd A terbium isotopes. With the present assignment both E1 transitions from the 481 keV level are forbidden by the asymptotic quantum number n_z [13]. Five time coincidence spectra between the 1.54 MeV β^--transition and the 481 keV gamma transition have been measured.

The window in the β channel was the same as in the previous measurement while the setting in the γ channel was shifted so as to suppress the influence from the strong 361 keV transition. A measured time coincidence distribution is shown in fig. 3. The main part of the curve is essentially prompt with a delayed tail caused by the 361 keV transition. Owing to the very high intensity of this line it is impossible to exclude its influence totally using plastic scintillators, with its inherently low energy resolution, and still retain some coincidence efficiency. The prompt peak is built up from the β^- 1.44 MeV - γ 529 keV cascade (~ 40 per cent) and the β^- 1.54 MeV - γ 481 keV cascade (~ 60 per cent). The slope of this part is about 0.2 ns. Momentum analysis of the above curve corrected for the delayed contribution gave in all cases time displacements less than 0.2 ns. From these evidences we conclude that both of the levels 586.1 keV and 480.6 keV have lifetimes less than 0.2 ns. This gives a hindrance factor of $< 1.3 \times 10^4$ and $< 1.5 \times 10^5$ for the two gamma rays of 165.3 keV and 482 keV , respectively, as compared with the Weisskopf estimate [1].

4.0 Discussion

Table 1 gives a summary of the experimental information used in calculating the transition probability P_γ (E1). A comparison with the Weisskopf estimate [1] through the retardation factor

$$F_W = \frac{P_\gamma(E1)(\text{exp})}{P(E1)(\text{Weisskopf})}$$

is also given. This factor varies between 10^3 - 10^6 in all these cases and shows that the actual E1 transitions are strongly retarded compared with the single particle Weisskopf estimate. In the region of strongly deformed nuclei, however, it is well known that better agreement with experiment is obtained when using a deformed potential as was orginally done by Nilsson [2]. He showed that the E1-transition probability between two single particle levels in a strongly deformed nucleus could be written as

$$P(E1) \approx 2.93 \cdot 10^{21}\left(1 - \frac{Z}{A}\right)^2 \left(\frac{E_\gamma}{197}\right)^3 A^{1/3} \cdot$$

$$\cdot \left[< I, 1, K, K' - K | I, 1, I', K' > \right]^2 \cdot \left\{ G_{E1} \right\}^2 \text{sec}^{-1} \qquad (2)$$

where

$$G_{E1} = \left\{ \sum_{\ell\ell'} < N'\ell' \mid r \mid N\ell > \cdot \sqrt{\frac{2\ell + 1}{2\ell' + 1}} \cdot < \ell, 1, 0, 0 | \ell, 1, \ell', 0 > \cdot \right.$$

$$\left. \cdot \sum_{\Lambda\Lambda'} \delta_{\Sigma\Sigma'} \cdot a_{\ell'\Lambda'} \cdot a_{\ell\Lambda} \cdot < \ell, 1, \Lambda, K' - K | \ell, 1, \ell', \Lambda' > \right\} \qquad (3)$$

Here E_γ is given in MeV and the prime denotes quantities belonging to the ground state. G_{E1} depends only on the intrinsic nature of the nucleus and can be calculated when the proper wave functions are known.

In order to compare the transition probability between similar levels in different nuclei, the experimental values of P_{E1} have been divided by the energy dependent factor before the brackets $\{ \ldots \}$ in eq. (2) and compared with the result from eq. (3) obtained with the Nilsson wave functions [2]. Table 2 gives the necessary information used in this calculation. In figs. 4 and 5 the theoretical G^2_{E1} factors are given as a function of the deformation parameter η, together with the experimental results. For the $\frac{3}{2}$ + (411) $\overrightarrow{\leftarrow}$ $\frac{5}{2}$ - (532) transitions the agreement with Nilsson's predictions is good, indicating a retardation factor of about 2. The matrix element for this transition is thus seen to be remarkably independent of the addition of even pairs of neutrons and protons. In the case of $\frac{5}{2}$ - (532) $\longrightarrow$ $\frac{5}{2}$ + (413), all experimental transition rates are faster than expected from the Nilsson theory. This is a situation which only seems to occur for E1 transitions with $\Delta K = 0$.

As was mentioned earlier, there are reasons to believe that the $\frac{5}{2}$ - (532) level, which is the ground state of Eu^{151} with a deformation of about $\delta \approx 0.15$, retains this low deformation even as an excited level in Eu^{153} and Eu^{155}. For this reason a calculation of the G^2_{E1} factor with decreasing η for the $\frac{5}{2}$ - (532) level has been performed.

The result is shown in figs. 4 and 5, which reveal that the G^2_{El} values increase as the deformation of the $\frac{5}{2}$ - (532) level decreases. This is in agreement with the result for the $\frac{5}{2}$ - (532) $\longrightarrow \frac{5}{2}$ + (413) transition, but seems to disagree with the $\frac{3}{2}$ + (411) $\rightleftarrows \frac{5}{2}$ - (532) transitions. There are, however, several other contributions to the transition probabilities which we have not taken into account. It is known that when the very short-range attractive forces not taken into account in the average field for the independent particle calculations are incorporated, this introduces a reduction factor to the transition probability. It can be shown [4] that for transitions near the ground state this reduction factor for the electric 2^L-pole transition [$\approx$ D(EL)] can be approximately given by

$$D(EL) \approx \frac{1}{2} \cdot \frac{E_\gamma}{E_\gamma + \Delta} \qquad (4)$$

where E_γ is the energy of the electro-magnetic transition and Δ is roughly given by the odd-even mass difference. The D(EL) value reduces the transition probability by approximately a factor of 20 to 5 in the energy range 100 to 500 keV, which is enough to compensate for the increased G^2_{El} values in the $\frac{3}{2}$ + (411) $\rightleftarrows \frac{5}{2}$ - (532) transitions, as the deformation of the $\frac{5}{2}$ - (532) level is lowered.

It is thus seen that to account for the transitions in the nuclei Eu^{153} and Eu^{155} one needs to assume that the $\frac{5}{2}$ - (532) state is associated with a radically smaller deformation. It would be interesting to see if the same assumption is necessary in Tb^{161}. For this heavier nucleus as born out by, e. g. for Tm^{169} in the calculations of Mottelson and Nilsson [13] the smaller deformation is no longer energetically competitive as it is for e. g. Eu^{153}.

References

1. WAPSTRA, A H, NIJGH, G J and VAN LIESHOUT, R,
Nuclear spectroscopy tables. North-Holland Publ, Amsterdam, 1959.

2. NILSSON, S G,
Binding states of individual nucleons in strongly deformed nuclei. Mat. Fys. Medd. Dan. Vid. Selsk 29 (1955) No. 16.

3. NATHAN, O and NILSSON, S G,
Collective nuclear motion and the unified model.
In "Alpha-beta and gamma ray spectroscopy", ed. by K. Siegbahn. North-Holland Publ, Amsterdam, 1964.

4. MALMSKOG, S G,
Absolute E1 transition probabilities in the deformed nuclei Yb^{177} and Hf^{179}. 1964 (AE-152)(submitted for publication in Nuclear Physics).

5. SUNDSTRÖM, T,
Note on moment analysis of delayed coincidence experiments. Nucl. Instr. and Meth. 16 (1962) 153.

6. POOL, M L and QUILL, L L,
Radioactivity induced in the rare earth elements by fast neutrons. Phys. Rev. 53 (1938) 437.

7. INGHRAM, M G, HAYDEN, R J and HESS, D C,
Activities induced by pile neutron bombardment of samarium. Phys. Rev. 71 (1947) 643.

8. RUTLEDGE, W C, CORK, J M and BURSON, S B,
Gamma-rays associated with selected neutron-induced radioactivities. Phys. Rev. 86 (1952) 775.

9. SCHMID, L C and BURSON, S B,
Decay of Sm^{155} (23.5 min). Phys. Rev. 115 (1959) 447.

10. SUND, R E, ARNS, R G and WIEDENBECK, M L,
Decay of Sm^{155}. Phys. Rev. 118 (1960) 776.

11. HARDELL, R and NILSSON, S,
Precision energy determination of isomeric levels and of low-lying excited states in deformed nuclei. Nuclear Physics 39 (1962) 286.

12. KRACIK, B, MILIGUI, Z et al.,
Decay of Sm^{155}. Czech. Journ. of Phys. 13 (1963) 79.

13. MOTTELSON, B R and NILSSON, S G,
The intrinsic states of odd-A nuclei having ellipsoidal equilibrium shape. Mat. Fys. Skr. Dan. Vid. Selsk 1 (1959) 8.

14. SUTER, T, REYES-SUTER, P et al.,
Decay of Sm^{153} to Eu^{153}. Nuclear Physics 29 (1962) 33.

15. SCHMID, L C, BURSON, S B and CORK, J M,
Decay of Gd^{161} (3.73 min). Phys. Rev. 115 (1959) 174.

16. HAMILTON, W D and DAVIES, K E,
The mean life and nuclear deformation of the 98 keV level in Eu^{153}. Nuclear Physics 58 (1964) 407.

17. GRAHAM, R L and WALKER, J,
The disintegration of Sm^{153}. Phys. Rev. 94 (1954) 794A.

18. GORODETSKY, S, MANQUENOUILLE, R, RICHERT, R and KNIPPER, A,
Periodes des niveaux excités a 362 keV du Tb^{159} et a 570 keV du Pb^{207}. J. Phys. Radium 22 (1961) 699.

Table 1

Experimental results E1 transitions between single particle levels

Transition	Nucleus	γ-ray energy in keV	Half life in 10^{-9} sec	M2 admixture	Total conversion coeff.	γ-ray intensity (%)	Experimental E1 transition probability P_γ (E1) sec^{-1}	$(G_{E1})^2$ from experiment	Retardation factor F_W	F_N
$\frac{5}{2}$ -(532)→ $\frac{5}{2}$ + (413)	Eu^{153}	97.4	0.16 [f]	< 2% [b]	0.40 [b]	99	3.0×10^{9}	6.4×10^{-3}	9.4×10^{2}	0.03
	Eu^{155}	104.4	< 0.2 [a]	< 2% [e]	0.43 [e]	100	$> 2.4 \times 10^{9}$	$> 4.2 \times 10^{-3}$	$< 1.4 \times 10^{3}$	< 0.05
	Tb^{161}	165.3	< 0.2 [a]	low [c]	0.11	32	$> 1.1 \times 10^{9}$	$> 4.6 \times 10^{-4}$	$< 1.3 \times 10^{4}$	< 0.46
$\frac{3}{2}$ +(411) $\rightleftarrows$ $\frac{5}{2}$ - (532)	Eu^{153}	75.4	0.14 [g]	< 2% [b]	0.48 [b]	3.2	$\sim 3 \times 10^{7}$	1×10^{-4}	4×10^{4}	1.8
	Eu^{155}	142	1.38 [a]	< 2% [e]	0.19	30	1.3×10^{8}	6.2×10^{-5}	6.5×10^{4}	2.7
	Tb^{159}	363	0.16 [h]	< 2%	< 0.02	97	4.3×10^{9}	1.2×10^{-4}	3.2×10^{4}	1.5
	Tb^{161}	482	< 0.2 [a]	low [d]	< 0.02	68	$> 2.3 \times 10^{9}$	$> 2.8 \times 10^{-5}$	$< 1.5 \times 10^{5}$	< 6.1
$\frac{7}{2}$ -(523)→ $\frac{5}{2}$ + (413)	Tb^{161}	102.4	0.84 [a]	low [c]	0.25	13	1.1×10^{8}	1.9×10^{-4}	3.0×10^{4}	5.5
$\frac{7}{2}$ -(523)→ $\frac{3}{2}$ + (411)	Tb^{161}	283.8	0.84 [a]	low [c]	0.05	10	8.0×10^{7}	K-forbidden	8.7×10^{5}	-
	Tb^{161}	361.0	0.84 [a]	low [c]	< 0.02	77	6.4×10^{8}	K-forbidden	2.3×10^{5}	-

a) present result
b) see ref. 14
c) see ref. 15
d) see discussion in the text
e) see ref. 9
f) see ref. 16
g) see ref. 17
h) see ref. 18

Table 2

Amplitudes of the Nilsson wave functions

Nucleus	Level energy and spin	Nilsson classification	Basic vectors $\|N\ell\Lambda\Sigma\rangle$	The amplitudes $a_{\ell\Lambda}$ normalized to $\sum_{\ell\Lambda} a^2_{\ell\Lambda} = 1$			δ a)
				$\eta = 2$	$\eta = 4$	$\eta = 6$	
Eu^{153}	97.4keV; $\frac{5}{2}$ -	$\frac{5}{2}$ - (532)	$\|552+\rangle$	0.8660	0.8727	0.8725	0.32
Eu^{155}	104.4keV; $\frac{5}{2}$ -		$\|532+\rangle$	0.1406	0.2435	0.3159	0.30
Tb^{159}	363 keV; $\frac{5}{2}$ -	No 36	$\|553-\rangle$	0.4739	0.4180	0.3656	0.31
Tb^{161}	480.6keV; $\frac{5}{2}$ -		$\|533-\rangle$	0.0460	0.0663	0.0724	0.30
Tb^{161}	417.6keV; $\frac{7}{2}$ -	$\frac{7}{2}$ - (523)	$\|553+\rangle$	0.9223	0.1446	0.9394	
			$\|533+\rangle$	0.0885	0.1446	0.1822	0.30
		No 35	$\|554-\rangle$	0.3763	0.3302	0.2903	
Eu^{153}	172.9keV; $\frac{5}{2}$ +	$\frac{3}{2}$ + (411)	$\|441+\rangle$	-0.3111	-0.4091	-0.4638	0.32
Eu^{155}	246 keV; $\frac{3}{2}$ +		$\|421+\rangle$	0.8704	0.8512	0.8407	0.30
Tb^{159}	0 keV; $\frac{3}{2}$ +	No 33	$\|442-\rangle$	0.1981	0.1800	0.1480	0.31
Tb^{161}	0 keV; $\frac{3}{2}$ +		$\|422-\rangle$	0.3261	0.2751	0.2369	0.30
Eu^{153}	0 keV; $\frac{5}{2}$ +	$\frac{5}{2}$ + (413)	$\|442+\rangle$	-0.3831	-0.3160	-0.2659	0.32
Eu^{155}	0 keV; $\frac{5}{2}$ +		$\|422+\rangle$	-0.2111	-0.2070	-0.1879	0.30
Tb^{161}	315.3keV; $\frac{5}{2}$ +	No 27	$\|443-\rangle$	0.8993	0.9251	0.9455	0.30

a) For the odd-proton nuclei in the region $50 < Z < 82$ the relation between the two deformation parameters δ and η is $\delta \sim 0.06\,\eta$.

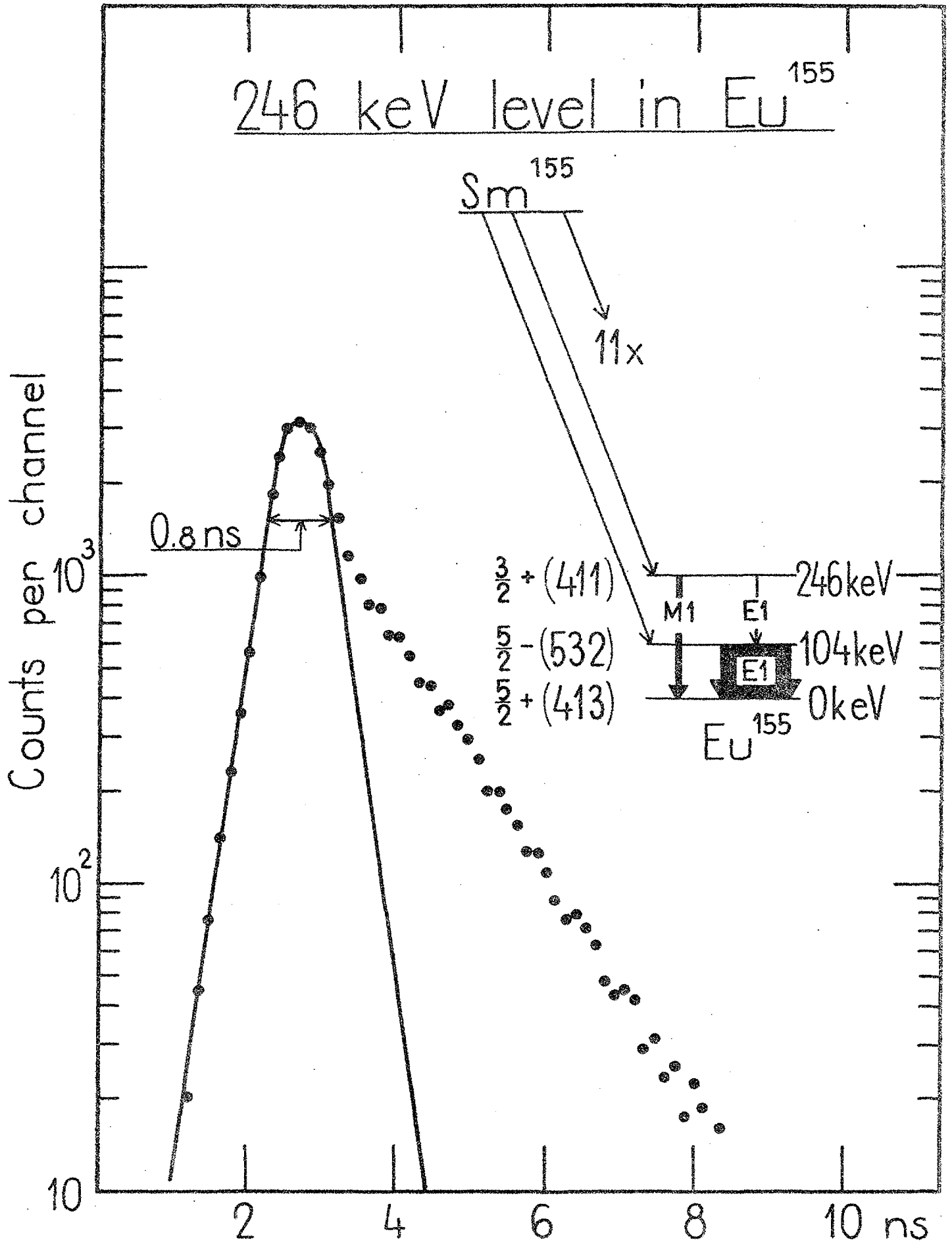

Fig. 1. Delayed coincidence curve taken between the continuous beta spectrum and the 245 keV gamma ray, giving a half life of 1.38 ± 0.06 ns for the 246 keV level in Eu^{155}.

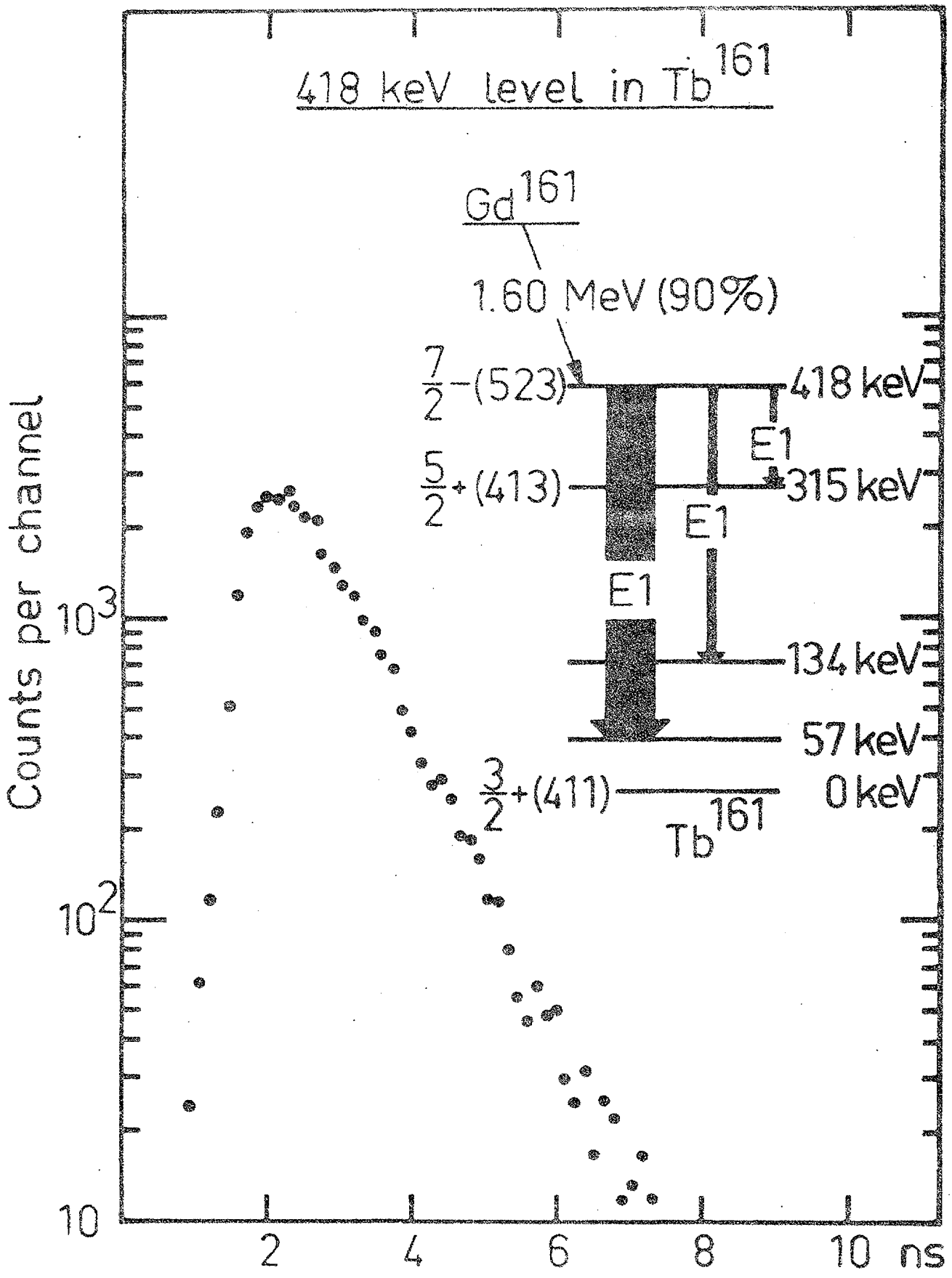

Fig. 2. Delayed coincidence curve taken between the continuous beta spectrum and the 361 keV gamma ray, giving a half life of 0.84 ± 0.04 ns for the 418 keV level in Tb^{161}. The inset shows a simplified decay scheme of Gd^{161} indicating the gamma transitions de-exciting the 418 keV level.

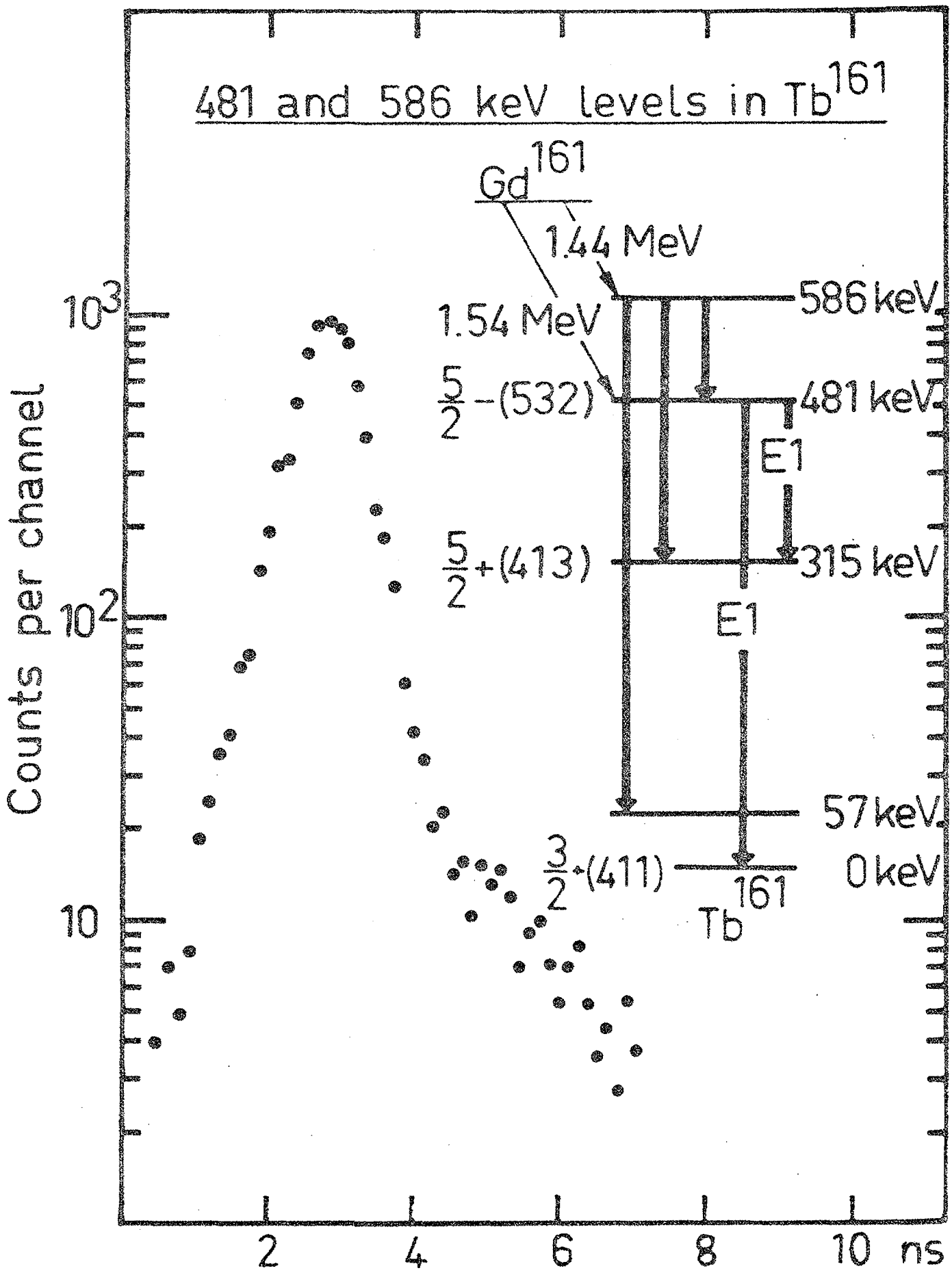

Fig. 3. Delayed coincidence curve taken between the continuous beta spectrum and a mixture of the 481 and 529 keV gamma rays, setting an upper limit of 0.2 ns for the half life of the 481 and 586 keV levels in Tb^{161}.

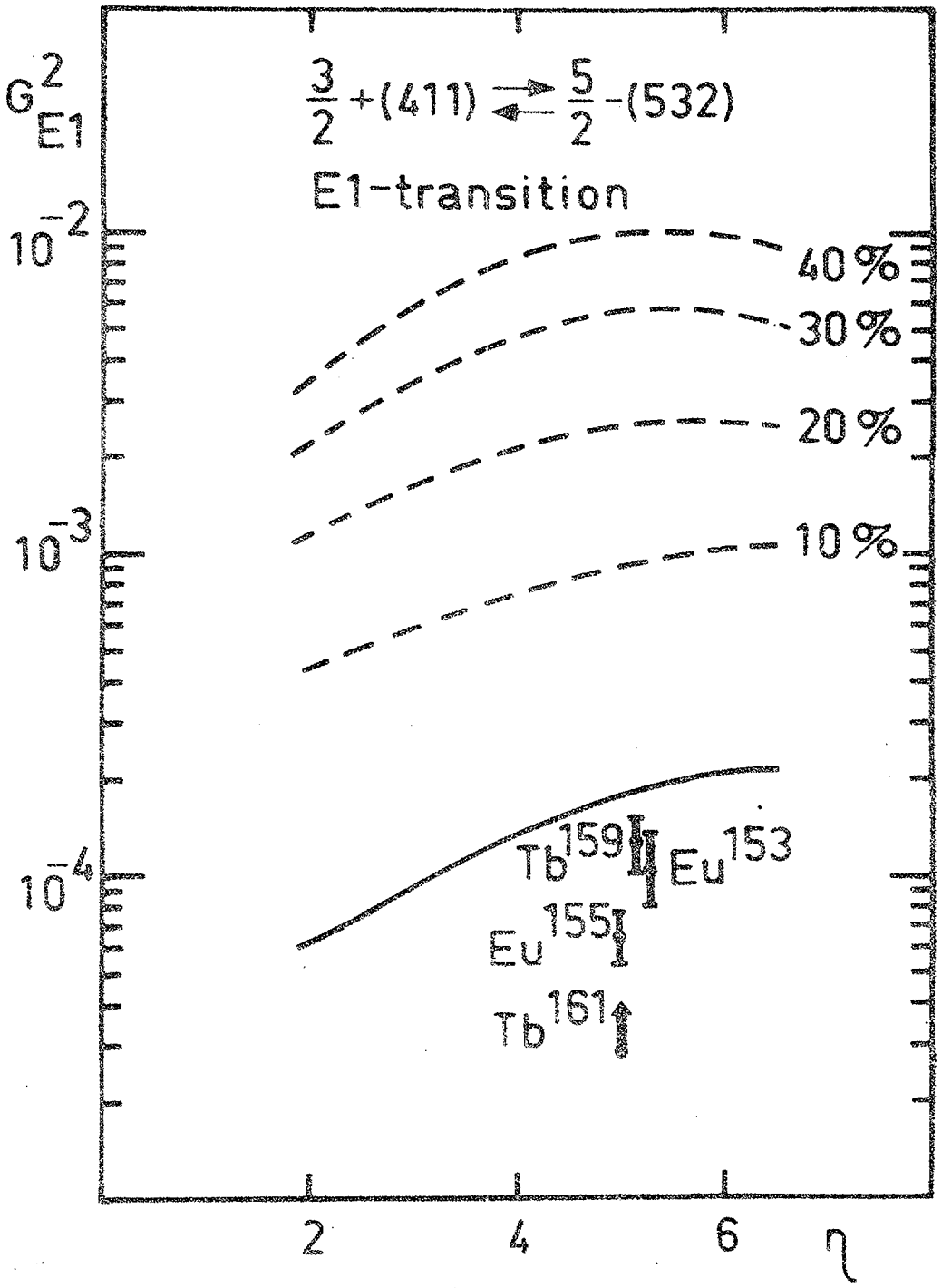

Fig. 4. Comparison between the $\frac{3}{2}$+ (411) ⇄ $\frac{5}{2}$ - (532) experimental and theoretical E1 transition probabilities.

——— shows the theoretical $(G_{E1})^2$-factor obtained from the Nilsson model (eq. 3) with the same deformation for the two levels.

---- with lower deformation (given in %) for the $\frac{5}{2}$ - (532) level.

● experimental values for the $(G_{E1})^2$-factor obtained from eq. 2.

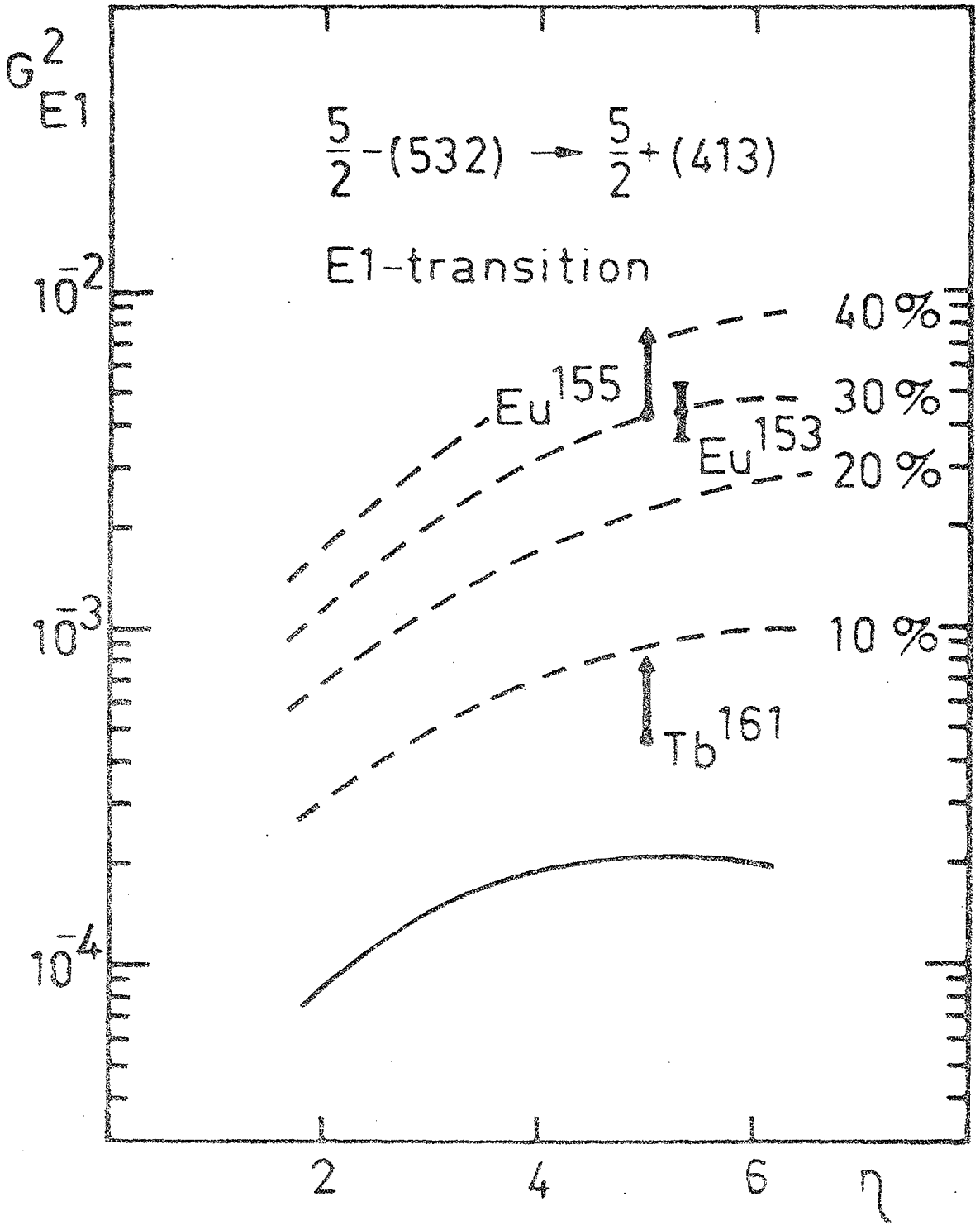

Fig. 5. Comparison between the $\frac{5}{2}$ - (532) → $\frac{5}{2}$ + (413) experimental and theoretical E1 transition probabilities.

——— shows the theoretical $(G_{E1})^2$-factor obtained from the Nilsson model (eq. 3) with the same deformation for the two levels.

----- with lower deformation (given in %) for the $\frac{5}{2}$ - (532) level.

● experimental values for the $(G_{E1})^2$-factor obtained from eq. 2.

LIST OF PUBLISHED AE-REPORTS

1—100. (See the back cover earlier reports.)

101. Solid angle computations for a circular radiator and a circular detector. By J. Konijn and B. Tollander. 1963. 6 p. Sw. cr. 8:—.

102. A selective neutron detector in the keV region utilizing the $^{19}F(n, \gamma)^{20}F$ reaction. By J. Konijn. 1963. 21 p. Sw. cr. 8:—.

103. Anion-exchange studies of radioactive trace elements in sulphuric acid solutions. By K. Samsahl. 1963. 12 p. Sw. cr. 8:—.

104. Problems in pressure vessel design and manufacture. By O. Hellström and R. Nilson. 1963. 44 p. Sw. cr. 8:—.

105. Flame photometric determination of lithium contents down to 10^{-3} ppm in water samples. By G. Jönsson. 1963. 9 p. Sw. cr. 8:—.

106. Measurements of void fractions for flow of boiling heavy water in a vertical round duct. By S. Z. Rouhani and K. M. Becker. 1963. 2nd rev. ed. 32 p. Sw. cr. 8:—.

107. Measurements of convective heat transfer from a horizontal cylinder rotating in a pool of water. K. M. Becker. 1963. 20 p. Sw. cr. 8:—.

108. Two-group analysis of xenon stability in slob geometry by modal expansion. O. Norinder. 1963. 50 p. Sw. cr. 8:—.

109. The properties of $CaSO_4Mn$ thermoluminescence dosimeters. B. Bjärngard. 1963. 27 p. Sw. cr. 8:—.

110. Semianolytical and seminumerical calculations of optimum material distributions. By C. I. G. Andersson. 1963. 26 p. Sw. cr. 8:—.

111. The paramagnetism of small amounts of Mn dissolved in Cu-Al and Cu-Ge alloys. By H. P. Myers and R. Westin. 1963. 7 p. Sw. cr. 8:—.

112. Determination of the absolute disintegration rate of Cs^{137}-sources by the tracer method. S. Hellström and D. Brune. 1963. 17 p. Sw. cr. 8:—.

113. An analysis of burnout conditions for flow of boiling water in vertical round ducts. By K. M. Becker and P. Persson. 1963. 28 p. Sw. cr 8:—.

114. Measurements af burnout conditions for flow of boiling water in vertical round ducts (Part 2). By K. M. Becker, et al. 1963. 29 p. Sw. cr. 8:—.

115. Cross section measurements of the $^{58}Ni(n, p)^{58}Co$ and $^{29}Si(n,\lambda m)^{26}Mg$ reactions in the energy range 2.2 to 3.8 MeV. By J. Konijn and A. Lauber 1963. 30 p. Sw. cr. 8:—.

116. Calculations of total and differential solid angles for a proton recoil solid state detector. By J. Konijn, A. Lauber and B. Tollander. 1963. 31 p. Sw. cr. 8:—.

117. Neutron cross sections for aluminium. By L. Forsberg. 1963. 32 p. Sw. cr. 8:—.

118. Measurements of small exposures of gamma radiation with $CaSO_4$:Mn radiothermoluminescence. By B. Bjärngard. 1963. 18 p. Sw. cr. 8:—.

119. Measurement of gamma radioactivity in o group of control subjects from the Stockholm area during 1959—1963. By I. Ö. Andersson, I. Nilsson and Eckerstig. 1963. 19 p. Sw. cr. 8:—.

120. The thermox process. By O. Tjölldin. 1963. 38 p. Sw. cr. 8:—.

121. The transistor as low level switch. By A. Lydén. 1963. 47 p. Sw. cr. 8:—.

122. The planning of a small pilot plant for development work on aqueous reprocessing of nuclear fuels. By T. U. Sjöborg, E. Haeffner and Hultgren. 1963. 20 p. Sw. cr. 8:—.

123. The neutron spectrum in a uranium tube. By E. Johansson, E. Jonsson, M. Lindberg and J Mednis. 1963. 36 p. Sw. cr. 8:—.

124. Simultaneous determination of 30 trace elements in cancerous and noncancerous human tissue samples with gamma-ray spectrometry. K. Samsahl, D. Brune and P. O. Wester. 1963. 23 p. Sw. cr. 8:—.

125. Measurement of the slowing-down and thermalization time of neutrons in water. By E. Möller and N. G. Sjöstrand. 1963. 42 p. Sw. cr. 8:—.

126. Report on the personnel dosimetry at AB Atomenergi during 1962. By K-A. Edvardsson and S. Hagsgård. 1963. 12 p. Sw. cr. 8:—.

127. A gas target with a tritium gas handling system. By B. Holmqvist and T. Wiedling. 1963. 12 p. Sw. cr. 8:—.

128. Optimization in activation analysis by means of epithermal neutrons. Determination of molybdenum in steel. By D. Brune and K. Jirlow. 1963. 11 p. Sw. cr. 8:—.

129. The P_1-approximation for the distribution of neutrons from a pulsed source in hydrogen. By A. Claesson. 1963. 18 p. Sw. cr. 8:—.

130. Dislocation arrangements in deformed and neutron irradiated zirconium and zircaloy-2. By R. B. Roy. 1963 18 p. Sw. cr. 8:—.

131. Measurements of hydrodynamic instabilities, flow oscillations and burnout in a natural circulation loop. By K. M. Becker, R. P. Mathisen, O. Eklind and B. Norman. 1964. 21 p. Sw. cr. 8:—.

132. A neutron rem counter. By I. Ö. Andersson and J. Braun. 1964. 14 p. Sw. cr. 8:—.

133. Studies of water by scattering of slow neutrons. By K. Sköld, E. Pilcher and K. E. Larsson. 1964. 17 p. Sw. cr. 8:—.

134. The amounts of As, Au, Br, Cu, Fe, Mo, Se, and Zn in normal and uraemic human whole blood. A comparison by means of neutron activation analysis. By D. Brune, K. Samsahl and P. O. Wester. 1964. 10 p. Sw. cr. 8:—.

135. A Monte Carlo method for the analysis of gamma radiation transport from distributed sources in laminated shields. By M. Leimdörfer. 1964. 28 p. Sw. cr. 8:—.

136. Ejection of uranium atoms from UO_2 by fission fragments. By G. Nilsson. 1964. 38 p. Sw. cr. 8:—.

137. Personnel neutron monitoring at AB Atomenergi. By S. Hagsgård and C-O. Widell. 1964. 11 p. Sw. cr. 8:—.

138. Radiation induced precipitation in iron. By B. Solly. 1964. 8 p. Sw. cr. 8:—.

139. Angular distributions of neutrons from (p, n)-reactions in some mirror nuclei. By L. G. Strömberg, T. Wiedling and B. Holmqvist. 1964. 28 p. Sw. cr. 8:.

140. An extended Greuling-Goertzel approximation with a P_n-approximation in the angular dependence. By R. Håkansson. 1964. 21 p. Sw. cr. 8:—.

141. Heat transfer and pressure drop with rough surfaces, a literature survey. By A. Bhattachayya. 1964. 78 p. Sw. cr. 8:—.

142. Radiolysis of aqueous benzene solutions. By H. Christensen. 1964. 40 p. Sw. cr. 8:—.

143. Cross section measurements for some elements suited as thermal spectrum indicators: Cd, Sm, Gd and Lu. By E. Sokolowski, H. Pekarek and E. Jonsson. 1964. 27 p. Sw. cr. 8:—.

144. A direction sensitive fast neutron monitor. By B. Antolkovic, B. Holmqvist and T. Wiedling. 1964. 14 p. Sw. cr. 8:—.

145. A user's manual for the NRN shield design method. By L. Hjärne. 1964. 107 p. Sw. cr. 10:—.

146. Concentration of 24 trace elements in human heart tissue determined by neutron activation analysis. By P. O. Wester. 1964. 33 p. Sw. cr. 8:—.

147. Report on the personnel Dosimetry at AB Atomenergi during 1963. By K.-A. Edvardsson and S. Hagsgård. 1964. 16 p. Sw. cr. 8:—.

148. A calculation of the angular moments of the kernel for a monatomic gas scatterer. By R. Håkansson. 1964. 16 p. Sw. cr. 8:—.

149. An anion-exchange method for the separation of P-32 activity in neutron-irradited biological material. By K. Samsahl. 1964. 10 p. Sw. cr. 8:—.

150. Inelastic neutron scattering cross sections of Cu^{6} and Cu^{65} in the energy region 0.7 to 1.4 MeV. By B. Holmqvist and T. Wiedling. 1964. 30 p. Sw. cr. 8:—.

151. Determination of magnesium in needle biopsy samples of muscle tissue by means of neutron activation analysis. By D. Brune and H. E. Sjöberg. 1964. 8 p. Sw. cr. 8:—.

152. Absolute E1 transition probabilities in the dofermed nuclei Yb^{177} and Hf^{179}. By Sven G. Malmskog. 1964. 21 p. Sw. cr. 8:—.

153. Measurements of burnout conditions for flow of boiling water in vertical 3-rod and 7-rod clusters. By K. M. Becker, G. Hernborg and J. E. Flinta. 1964. 54 p. Sw. cr. 8:—.

154. Integral parameters of the thermal neutron scattering law. By S. N. Purohit. 1964. 48 p. Sw. cr. 8:—.

155. Tests of neutron spectrum calculations with the help of foil measurments in a D_2O and in an H_2O-moderated reactor and in reactor shields of concrete and iron. By R. Nilsson and E. Aalto. 1964. 23 p. Sw. cr. 8:—.

156. Hydrodynamic instability and dynamic burnout in natural circulation two-phase flow. An experimentol ond theoretical study. By K. M. Becker, S. Jahnberg, I. Haga, P. T. Hansson and R. P. Mathisen. 1964. 41 p. Sw. cr. 8:—.

157. Measurements of neutron and gamma attenuation in massive laminated shields of concrete and a study of the accuracy of some methods of calculation. By E. Aalto and R. Nilsson. 1964. 110 p. Sw. cr. 10:—.

158. A study of the angular distributions of neutrons from the Be^{9} (p,n) B^{9} reaction at low proton energies. By B. Antolkovic', B. Holmqvist and T. Wiedling. 1964. 19 p. Sw. cr. 8:—.

159. A simple apparatus for fast ion exchange separations. By K. Samsahl. 1964. 15 p. Sw. cr. 8:—.

160. Measurements of the Fe^{54} (n, p) Mn^{54} reaction cross section in the neutron energy range 2.3—3.8 MeV. By A. Lauber and S. Malmskog. 1964. 13 p. Sw. cr. 8:—.

161. Comparisons of measured and calculated neutron fluxes in laminated iron and heavy water. By E. Aalto. 1964. 15 p. Sw. cr. 8:—.

162. A needle-type p-i-n junction semiconductor detector for in-vivo measurement of beta tracer activity. By A. Lauber and B. Rosencrantz. 1964. 12 p. Sw. cr. 8:—.

163. Flame spectro photometric determination of strontium in water and biological material. By G. Jönsson. 1964. 12 p. Sw. cr. 8:—.

164. The solution of a velocity-dependent slowing-down problem using case's eigenfunction expansion. By A. Claesson. 1964. 16 p. Sw. cr. 8:—.

165. Measurements of the effects of spacers on the burnout conditions for flow of boiling water in a vertical annulus and a vertical 7-rod cluster. By. K. M. Becker end G. Hernberg. 1964. 15 p. Sw. cr. 8:—.

166. The transmission of thermal and fast neutrons in air filled annular ducts through slabs of iron and heavy water. By J. Nilsson and R. Sandlin. 1964. 33 p. Sw. cr. 8:—.

167. The radio-thermoluminescense of $CaSO_4$: Sm and its use in dosimetry. By B. Bjärngard. 1964. 31 p. Sw. cr. 8:—.

168. A fast radiochemical method for the determination of some essential trace elements in biology and medicine. By K. Samsahl. 1964. 12 p. Sw. cr. 8:—.

169. Concentration of 17 elements in subcellular fractions of beef heart tissue determined by neutron activation analysis. By P. O. Wester. 1964. 29 p. Sw. cr. 8:—.

170. Formation of nitrogen-13, fluorine-17, and fluorine-18 in reactor-irradiated H_2O and D_2O and applications to activation analysis and fast neutron flux monitoring. By L. Hammar and S. Forsén. 1964. 25 p. Sw. cr. 8:—.

171. Measurements on background and fall-out radioactivity in samples from the Baltic bay of Tvären, 1957—1963. By P. O. Agnedal. 1965. 48 p. Sw. 8:—.

172. Recoil reactions in neutron-activation analysis. By D. Brune. 1965. 24 p. Sw. cr. 8:—.

173. A parametric study of a constant-Mach-number MHD generator with nuclear ionization. By J. Braun. 1965. 23 p. Sw. cr. 8:—.

174. Improvements in applied gamma-ray spectrometry with germanium semiconductor dector. By D. Brune, J. Dubois and S. Hellström. 1965. 17 p. Sw. cr. 8:—.

175. Analysis of linear MHD power generators. By E. A. Witalis. 1965. 37 p. Sw. cr. 8:—.

176. Effect of buoyancy on forced convection heat transfer in vertical channels — a literature survey. By A. Bhattacharyya. 1965. 27 p. Sw. cr. 8:—.

179. Hindered E1 transitions in Eu^{155} and Tb^{161}. By S. G. Malmskog. 1965. 19 p. Sw. cr. 8:—.

Förteckning över publicerade AES-rapporter

1. Analys medelst gamma-spektrometri. Av D. Brune. 1961. 10 s. Kr 6:—.
2. Beströlningsförändringar och neutronatmosfär i reaktortrycktankar — några synpunkter. Av M. Grounes. 1962. 33 s. Kr 6:—.
3 Studium av sträckgränsen i mjukt stål. Av G. Östberg och R. Attermo. 1963. 17 s. Kr 6:—.
4. Teknisk upphandling inom reaktorområdet. Av Erik Jonson. 1963. 64 s. Kr. 8:—.
5. Agesta Kraftvärmeverk. Sammanställning av tekniska data, beskrivningar m. m. för reaktordelen. Av B. Lilliehöök. 1964. 336 s. Kr. 15:—.

Additional copies available at the library of AB Atomenergi, Studsvik, Nyköping, Sweden. Transparent microcards of the reports are obtainable through the International Documentation Center, Tumba, Sweden.

EOS-tryckerierna, Stockholm 1965